Cancer Heterogeneity and Plasticity
https://doi.org/10.47248/chp2603010003

Original Research

YAP1 depletion enhances TAZ and its complexation with TEAD4 and AP-1 heterodimer C-JUN/FOSB in gastric cancer progression and metastasis

Jingjing Wu [1,2], Dipti Athavale [3,4], Curt Balch [3,4], Junsong Zhao [3,4], Gengyi Zou [1], Yibo Fan [1], Yanting Zhang [3,4,5], Joseph Zhao [6], Mikel Ghelfi [3,4], Anthony Pompetti [3,4], Gennaro Calendo [3,4], Ailing Scott [1], Shan Shao [1], Xiaodan Yao [3,4], Melissa Pool Pizzi [1], Christopher Vellano [7], Vladimir Khazak [8], Sheng Zhang [2], Timothy A Yap [9], Shilpa S Dhar [1], Raghav Sundar [6], Francis Spitz [4,5,10], Generosa Grana [4,10], Jaffer A. Ajani [1,*], Shumei Song [3,4,5,10,11,*]

Cite This Article:
Wu J, Athavale D, Balch C, Zhao J, Zou G, Fan B, Zhang Y, Zhao J, Ghelfi M, Pompetti A, Calendo G, Scott A, Shao S, Yao X, Pizzi M P, Vellano C, Khazak V, Zhang S, Yap T A, Dhar S S, Sundar R, Spitz F, Grana G, Ajani J A, Song S. YAP1 depletion Enhances TAZ and its complexation with TEAD4 and AP-1 heterodimer C-JUN/FOSB in gastric cancer progression and metastasis. Cancer Heterog Plast. 2026;3(1):0003. https://doi.org/10.47248/chp2603010003

Received: 16 Jan 2026
Accepted: 17 Mar 2026
Published: 28 Mar 2026

1. Department of GI Medical Oncology, The University of Texas MD Anderson Cancer Center, Houston, TX 77030, USA; Emails: 4468726@qq.com (J.W); GZou@mdanderson.org (G.Z.); yfan25@central.uh.edu (Y.F.); awscott@mdanderson.org (A.S.); SShao@mdanderson.org (S.S.); mppizzi@mdanderson.org (M.P.P.); SSDhar@mdanderson.org (S.S.D.)
2. Department of Pathology, The First Affiliated Hospital of Fujian Medical University, Fuzhou, Fujian 350005, China; Email: zhgshg@126.com (S.Z.)
3. Coriell Institute for Medical Research, 403 Haddon Ave, Camden, NJ, 08103, USA; Emails: dathavale@coriell.org (D.A.); cbalch@coriell.org (C.B.); jzhao@coriell.org (J.Z.); yzhang@coriell.org (Y.Z.); mghelfi@coriell.org (M.G.); apompetti@coriell.org (A.P.); gcalendo@coriell.org (G.C.); xyao@coriell.org (X.Y.)
4. Camden Cancer Research Center, 403 Haddon Ave, Camden, NJ, 08103, USA; Emails: Spitz-Francis@cooperhealth.edu (F.S.); grana-generosa@cooperhealth.edu (G.G.)
5. Departments of Biomedical Sciences and Surgery, Cooper Medical School of Rowan University, 401 Broadway, Camden, NJ, 08103, USA
6. Department of Medicine, Yale School of Medicine and Yale Cancer Center, PO Box 208028, New Haven, CT 06520-8028, USA; Emails: joseph.zhao@yale.edu (J.Z.); raghav.sundar@yale.edu (R.S.)
7. Therapeutics Discovery Division, The University of Texas MD Anderson Cancer Center, Houston, TX 77030, USA; Email: CPVellano@mdanderson.org (C.V.)
8. NexusPharma Inc. 17 Black Forest Road, Hamilton, NJ 08691, USA; Email: vladimir.khazak@gd3services.com (V.K.)
9. Department of Investigational Cancer Therapeutics (Phase 1 program), The University of Texas MD Anderson Cancer Center, Houston, TX 77030, USA; Email: TYap@mdanderson.org (T.A.P.)
10. MD Anderson Cancer Center at Cooper, Cooper University Hospital, 2 Cooper Plaza, Camden, NJ, 08103, USA
11. Department of Cancer Pharmacology, Rutgers Cancer Institute, 195 Little Albany St, New Brunswick, NJ 08901, USA

* **Correspondence:** Shumei Song; Email: ssong@coriell.org; Jaffer A. Ajani; Email: jajani@mdanderson.org

Abstract

Background Dysregulation of the Hippo signaling pathway, characterized by aberrant activation of the transcriptional coactivators YAP1 and TAZ, drives tumor progression, immunosuppression, and metastasis. Hippo pathway components are emerging therapeutic targets in several solid tumors, however, the expression profiles of Hippo coactivators YAP1, TAZ, and their transcriptional factors TEAD1-4 in gastric cancer peritoneal metastases (GCPMs), and their therapeutic value, are unknown. In this study, we sought to determine the expression status of YAP1, TAZ, and TEAD1-4 in GCPMs and to evaluate whether dual targeting of YAP1 and TAZ provides superior antitumor activity compared with inhibition of either coactivator alone.

Methods Expression of YAP1, TAZ, and TEAD1–4 was examined in GCPMs by single-cell RNA sequencing and co-immunofluorescent staining. Functional studies using genetic knockout and antisense oligonucleotide (ASO) inhibition of YAP1 or TAZ were performed to assess antineoplastic effects *in vitro* and *in vivo*. Co-immunoprecipitation and luciferase reporter assays were used to characterize YAP1/TAZ interactions with TEADs and AP-1 components (JUN and FOSB) and to quantify transcriptional activity. Antitumor efficacy was validated in patient-derived xenograft (PDX) and KP-Luc2 syngeneic models.

Results YAP1, TAZ, and TEADs1- 4 were highly coexpressed in GCPMs and correlated with poor survival. YAP1 inhibition alone elicited compensatory upregulation of TAZ, while combined inhibition of both coactivators maximally repressed cell proliferation and invasion *in vitro*, and tumor growth *in vivo*. Increased TAZ complexation with TEAD4 and AP-1 (c-JUN and FOSB) heterodimer was observed following YAP1 knockdown or pharmacological ASO inhibition. Dual inhibition of YAP1 and TAZ was required to maximally suppress YAP1/TAZ expression and reduce their nuclear accumulation, transactivation of TEAD, and activation of downstream genes.

Conclusions These findings show that combined YAP1 and TAZ inhibition holds promise for the treatment of GCPM, a highly lethal disease with an urgent need for novel treatment options.

Keywords: Antisense oligonucleotide (ASO), gastric cancer peritoneal metastasis (GCPM), Hippo pathway, YAP1, TAZ, TEAD1-TEAD4, targeted therapy

1. Introduction

Gastric cancer (GC) is the fifth-leading cause of cancer, worldwide, and the fourth-leading cause of cancer death [1]. In the U.S. alone, the American Cancer Society estimates 30,300 new gastric cancer cases in 2025, with 10,780 deaths [2,3]. Primary causes of GC include *Helicobacter Pylori* infection, male gender, advanced age, consumption of smoked/salted meats, and tobacco use [4]. Approximately 45% of GC patients present with peritoneal metastases (PMs, malignant ascites or implants in the peritoneal cavity), having a five-year survival rate of merely 6% [1]. Our group previously reported that GC with PM

(GCPM) is predominantly driven by Hippo/YAP1 signaling, and that YAP1 inhibition is strongly antineoplastic and suppresses GCPM [5].

The complexity of cancer involves intricate signaling pathways that regulate cell growth, proliferation, cell fate decisions, and tissue homeostasis. Among these pathways is the highly conserved Hippo pathway, a critical regulator of organ size, tissue regeneration, stem cell self-renewal, and tumorigenesis through its co-activators Yes-associated protein 1 (YAP1) and transcriptional co-activator with PDZ-binding motif (TAZ) that interact with the transcription factors TEAD1-TEAD4 [6]. YAP1 and TAZ are encoded by paralogous genes, with 46% amino acid identity [7].

Central to Hippo function is a series of kinases and transcriptional co-activators that coordinate cellular responses to various cues, including cell-cell contact, mechanotransduction, and soluble factors. Under homeostatic conditions, YAP1 and TAZ are phosphorylated by the Hippo kinase LATS 1/2 (large tumor suppressor kinases) and sequestered in the cytoplasm by 14-3-3-σ proteins or degraded [7]. Since YAP1/TAZ are mitogenic effectors, cytoplasmic sequestration/degradation effectively constrains cell growth. Under dysregulated conditions (as in various cancers), however, phosphorylation (and thus, Hippo signaling) is disrupted, resulting in YAP1 or TAZ nuclear translocation and interaction with the TEA domain (TEAD) transcription factors TEAD1-TEAD4, activating genes involved in stemness, proliferation, epithelial-to-mesenchymal transition (EMT), angiogenesis, and therapy resistance [8]. Adding additional complexity, YAP1 and TAZ can crosstalk with other signaling pathways such as Wnt/β-catenin, AP-1, Notch, STAT3, and TGF-β, amplifying their oncogenic potential and ability to form a permissive microenvironment for tumor progression [7,9-13].

Although YAP1 and TAZ are thought to be largely functionally redundant, the degree of overlap, in association with cancer phenotypes, remains unclear [7,9,12-14]. For example, in hepatocellular cancer (HCC), TAZ knockdown resulted in increased YAP1 levels, concomitant with increased cancer stem cell traits (therapy-resistance and tumorigenicity), and combined YAP1/TAZ inhibition was found most efficacious in tumor suppression [15]. Likewise, during embryonic development, only combined inhibition of YAP1 and TAZ could completely halt blastocyst formation, whereas inhibition of either factor alone was insufficient. These observations suggest that Hippo-pathway strategies centered solely on YAP1 inhibition may be inadequate because of compensatory signaling through TAZ. Consistent with this possibility, a recent clinical trial (NCT04659096) evaluating YAP1 antisense oligonucleotide (ASO) therapy in advanced solid tumors did not succeed; however, the basis for this failure and the potential compensatory activation of TAZ and its binding partners in GCPMs remain unknown. Together, these findings underscore the novelty and rationale of our current study comparing dual *versus* single targeting of YAP1 and its TAZ paralog in GCPMs.

In this study, we extensively characterized the expression of YAP1 and TAZ and their transcription factors TEAD1-TEAD4 in advanced GCPM samples; both YAP1 and TAZ interacted with TEAD1-TEAD4 to enhance TEAD transcriptional activity. Further, we found that YAP1 or TAZ ASOs efficiently knocked down YAP1 or TAZ, respectively, *in vitro*. Moreover, we show that genetic knockout (KO) or pharmacological inhibition of YAP1 enhanced TAZ expression and activity,

strengthened TAZ–TEAD4 binding, and promoted TAZ interaction with the AP-1 heterodimer (c-JUN/FOSB). Consequently, combined ASO inhibition of YAP1 and TAZ was necessary to maximally suppress both invasion and proliferation *in vitro* and suppress tumor growth *in vivo*. Together, these findings indicate that co-targeting both Hippo pathway effectors may offer greater therapeutic benefit than inhibiting either one alone.

2. Materials and Methods

2.1. Sex as a biological variable

Our study examined both male and female animals; similar findings are reported for both sexes.

2.2. Cells and reagents

The human gastric cancer cell line AGS was purchased from the American Type Culture Collection (ATCC, Manassas, VA). GA0518 and GA0804 are patient-derived cells isolated from ascites or patient-derived xenograft (PDX) tumors from gastric cancer (GC) specimens and were described previously [16]. The KP-Luc2 murine GAC cell line was from Dr. Jo Ishizawa in the Department of Leukemia of MDACC and was previously reported [17]. All cell lines were authenticated and profiled biannually by the Cell Line Core Facility at The University of Texas MD Anderson Cancer Center. YAP1 antisense oligonucleotides (ASOs) and TAZ ASOs were sourced from Ionis Pharmaceuticals, Inc. (Carlsbad, CA). ASOs were initially dissolved in dimethyl sulfoxide (DMSO) at a concentration of 10 mM, with aliquots stored at -20°C. Fresh working solutions were prepared as required for each experiment. PCR primers used in the study are listed in **Table S1**, and antibodies and their sources are listed in **Table S2**.

2.3. Isolation of GCPM cells from malignant ascites of GC patients

Malignant ascites (100 mL to 2000 mL) was collected under an IRB-approved protocol (Lab01-543) at MDACC and CCCB0001 of the Cooper-Coriell Cancer Biobank at the Camden Cancer Research Center (CCRC), respectively. Cytology was confirmed by two clinical pathologists (R.W & D.C). Ascites was centrifuged at 2000 rpm for 20 min, and centrifuged GCPM cells and supernatants processed and stored. Cell pellets were resuspended in RPMI1640 + 5% FBS + 1% Pen/Strep and red blood cells (RBCs) lysed in RBC lysis buffer. GCPM cell pellets were fixed, placed in cell blocks, and sectioned for evaluation of markers by IHC and Co-IF. Live cells with 10% DMSO were stored in liquid nitrogen for later flow cytometry and scRNA-seq.

2.4. Lentiviral transfection and establishment of stable cell lines

YAP1 knockout cells were generated from the GA0518 cell line using the LentiCRISPR/Cas9 system. Briefly, gRNAs targeting YAP1 were designed using the MIT CRISPR Design Tool (http://crispr.mit.edu/). These gRNAs were cloned into the pLentiCRISPR v1 vector (GeCKO LentiCRISPR resource, MIT; http://genome-engineering.org/gecko/), using BsmBI digestion. The vector backbone, containing the Cas9 gene, was ligated with gRNA duplexes, and successful clones were verified by sequencing. Lentivirus was produced in HEK293T cells cultured in six-well plates by cotransfecting the pLentiCRISPR-gRNA construct with packaging plasmids pCMV.Dr8.2 and pCMV.VSV.G at a ratio

of 10:10:1. Lentiviral supernatant was used to transduce GA0518 cells expressing mCherry-Luciferase in six-well plates, supplemented with 8 μg/ml polybrene. Transduced cells were selected with puromycin at appropriate concentrations for 1-2 weeks to establish stable YAP1 knockout lines. Cells were subsequently propagated, and knockout efficiency was confirmed by Western blot analysis.

2.5. Co-immunoprecipitation assays

Co-immunoprecipitation (Co-IP) assays were performed using the Thermo Scientific™ Pierce™ Classic Magnetic IP/Co-IP Kit (#88804), according to the manufacturer's instructions. Briefly, prepared cell lysates were incubated overnight at 4°C with antibodies against: TAZ (Novus, Wrentham, MA, NBP1-85067), YAP1 (Cell Signaling Technology, Danvers, MA, #14074), TEAD1 (Cell Signaling Technology, #12292), TEAD2 (MilliporeSigma, Burlington, MA, Cat#SAB4503373), TEAD3 (Abcam, Cambridge, UK, #ab75192), TEAD4 (Abcam, #58310), c-JUN (Cell Signaling Technology, #9615), or FOS-B (Cell Signaling Technology, #2251). Protein A/G magnetic beads were then added to the lysate-antibody mixtures and incubated for 1 h at room temperature to capture immune complexes. Beads were washed twice with IP Lysis/Wash Buffer and once with purified water to remove unbound proteins. Finally, antigen-antibody complexes were eluted from the beads for downstream analysis. Antibody concentrations used for subsequent Western blotting matched those employed in standard Western blot assays.

2.6. Western blotting

Proteins were extracted from whole-cell lysates using RIPA buffer. Protein concentration was quantified using a BCA Protein Assay Kit (Thermo Fisher Scientific, Waltham, MA), according to the manufacturer’s instructions, with bovine serum albumin (BSA) as the standard. Equal amounts of protein were separated by 10% polyacrylamide gel electrophoresis (SDS-PAGE) and transferred to PVDF membranes using a Trans-Blot® Turbo™ Transfer System (Bio-Rad, Hercules, CA). Membranes were incubated with the designated primary antibodies overnight at 4°C, followed by incubation with appropriate horseradish peroxidase (HRP)-conjugated secondary antibodies. Protein bands were visualized using ECL Western Blotting Detection Reagent (Thermo Fisher Scientific) via chemiluminescence. The following primary antibodies and dilutions were used: YAP1 (1:1000), TAZ (1:1000), TEAD1 (1:1000), TEAD2 (1:1000), TEAD3 (1:1000), TEAD4 (1:1000), Survivin (1:1000), Snail (1:500), and β-actin (1:10,000).

2.7. YAP/TEAD luciferase reporter assay

YAP1/TEAD transcriptional activity was assessed using the Dual-Luciferase Reporter Assay System (Promega, Madison, WI). AGS, GA051816, and GA080417 cells were transiently co-transfected with UAS-luciferase and Gal4-TEAD plasmids, along with a Renilla luciferase vector as an internal control. For specific experimental conditions, a human YAP1 overexpression vector was also co-transfected. Eight hours post-transfection, cells were treated with various concentrations of antisense oligonucleotides (ASOs) or vehicle control for 24 h. Luciferase activity was then measured using a luciferase assay kit (Promega). Firefly luciferase activity was normalized to Renilla luciferase activity to account for transfection efficiency variations. Transfection

experiments were independently performed at least three times, with each condition assayed in triplicate.

2.8. Immunofluorescent staining

Immunofluorescence staining was performed as previously described [5]. Antigen retrieval was conducted using Antigen Unmasking Solution (BioGenex Laboratories, Fremont, CA). The following primary antibodies were applied at the indicated dilutions: YAP1 (Cell Signaling Technology, #14074, 1:100), TAZ (Novus, NBP1-85067; 1:100); Ki67 (Thermo Fisher Scientific, #RM-9106-S1, 1:150), TEAD1 (Cell Signaling Technology, #12292, 1:100), TEAD2 (SAB4503373; 1:100), TEAD3 (Abcam, ab75192; 1:100), TEAD4 (Abcam, #58310, 1:100), CD8 (Cell Signaling Technology, #98941, 1:100), CD206 (Abcam, #64693, 1:100). Slides were mounted using Vectashield Mounting Medium with DAPI (Vector Laboratories, Newark, CA) and visualized under a Nikon A1 confocal laser scanning microscope.

2.9. Colony formation assay

GA051816 gastric cancer (GC) cells were seeded in six-well plates at a density of 800 cells per well (optimized to yield countable colonies). Cells were treated with YAP1 ASO, TAZ ASO, or a combination of YAP1 ASO + TAZ ASO at indicated concentrations. After 10–14 days of culture, colonies were fixed with 3% crystal violet in 10% formalin. Colonies containing >50 cells were counted, and clonogenic survival fraction was calculated. All treatments were performed in at least triplicate.

2.10. Transwell migration assay

Migration assays were performed using 24-well Transwell® plates with 8.0-μm pore inserts (Corning, Corning, NY). The lower chamber contained 750 μL of RPMI-1640 medium supplemented with 20% FBS. Target cells (1×10^5) in RPMI-1640 medium with 1% FBS were seeded in the upper chamber. YAP1 ASO or TAZ ASO was added at specified concentrations. Plates were incubated at 37°C for 24 h. Non-migrated cells on the upper surface were removed by scraping. Migrated cells on the filter's lower surface were fixed with 10% formalin and stained with 0.5% crystal violet. Images from the transwell migration assay were captured and analyzed using the 'Analyze Particles' function in ImageJ software (NIH, Bethesda, MD), where colony counts per well were calculated automatically. Migrated cells on the filter's lower side were quantified by counting five randomly selected fields under a microscope at 20× magnification. Each assay was performed in triplicate.

2.11. RT-qPCR

Total RNA was extracted from cells or tissues using TRIzol™ reagent (Thermo Fisher Scientific). RNA concentration and purity were assessed by spectrophotometry (NanoDrop). Reverse transcription was performed using the LunaScript® RT SuperMix Kit (New England Biolabs, Beverly, MA), according to the manufacturer's protocol. RT-qPCR was performed on the cDNA using SYBR Green Master Mix (Applied Biosystems, Carlsbad, CA). Gene expression levels were normalized to GAPDH expression using the $2^{-\triangle\triangle Ct}$ method. Each assay was conducted in triplicate. Primer sequences are shown in **Table S1**.

2.12. Single cell RNA sequencing (sc-RNA Seq) analysis

Droplet-based 3'-single-cell RNA-Seq (10x Genomics, Pleasanton, CA) was performed on ascites samples (n = 20) at the SMF core at MD Anderson Cancer Center as described [18]. In brief, transcripts were mapped, assigned to individual cells by barcodes using Cell Ranger, and analyzed using Seurat in R 3.5.0. Genes with detected expression in at least 3 cells, and cells with at least 200 genes detected were used. The first 15 Principal Components were used for clustering (resolution = 0.6). For RNA sequencing analysis, total RNA was isolated using a miRNeasy Mini Kit (Qiagen, Germantown, MD), according to the manufacturer's protocol, from all ascites cells. Only RNA with more than 7 of RNA integrity number was sent to the DNA core for RNA Sequencing. The raw RNA-sequencing (RNA-seq) readouts were mapped to the human GRCh38 assembly reference genome using TopHat2, an open-source software tool that aligns RNA-seq reads to a reference genome. Heatmaps were generated with unsupervised clustering and differential gene expression analyses performed with DESeq2 (R/Bioconductor package) using adjusted p values < 0.05 as the significance cutoff.

2.13. Immunohistochemistry

Immunohistochemistry (IHC) for YAP1 or TAZ was performed on human tissue microarray slides consisting of samples of around 390 gastric tumor tissues and non-neoplastic gastric tissues from patients that underwent total or subtotal gastrectomy for GC between January 2006 and December 2008 at the First Affiliate Hospital of China Medical University. Written informed consent was obtained from all patients, and all patients were followed up via telephone inquiry or questionnaires. Antibodies for YAP1 are described previously [5]. Sections were incubated with primary human YAP1 (Cell Signaling, cat#14074; 1:100) and human TAZ (Novus, cat#NBP1-85067; 1:100) antibodies, followed by biotinylated secondary antibodies and a streptavidin HRP kit (Vector Laboratories, PK-6100). IHC score was based on criteria from our previous study [5,19,20].

2.14. The PDX and KP-Luc2 syngeneic mouse models

Ten- to twelve-week-old SCID mice were subcutaneously inoculated with GA051816 cells (2×10^6 cells/mouse; n = 5 per group). For the YAP1/TAZ ASO efficacy study, treatment commenced 15 days post-inoculation when xenografts were established. Mice received intraperitoneal injections of: YAP1 ASO (40 mg/kg), TAZ ASO (40 mg/kg), their combination (YAP1 ASO 20 mg/kg + TAZ ASO 20 mg/kg), or PBS vehicle control (100 µL/mouse). Treatments were administered five times weekly for three consecutive weeks.

Using the KP-Luc2 syngeneic model, established KP-Luc2 xenograft-bearing mice were treated with YAP1 ASO monotherapy (40 mg/kg), anti-PD-1-neutralizing antibody (Bio X Cell; Cat# BE0146-R-100mg; 10 mg/kg, IP), combination therapy (YAP1 ASO 40 mg/kg + anti-PD-1 10mg/kg), or PBS control, 5 times a week for a total of 3 weeks. Tumor volumes (calculated as length × $\text{width}^2 \times 0.5$), tumor weights, and body weights were monitored throughout the study period, as previously described [21].

2.15. Statistical analyses

All statistical analyses were conducted using SPSS software (version 20.0; IBM Corp.). Continuous data are presented as mean ± standard deviation (SD) or

standard error of the mean (SEM), as specified in the figure legends. For comparisons between two independent groups, we employed unpaired two-tailed Student's t-tests after verifying the assumptions of normality and homogeneity of variance. The threshold for statistical significance was established *a priori* at $p < 0.05$ for all analyses. T-SNE clustering of scRNA-seq data was performed using the sci-kit-learn machine learning library. The specific sample size for each experimental condition is provided in the respective figure legends. All statistical tests were selected based on the experimental design and data characteristics, with appropriate validation of test assumptions.

3. Results

3.1. YAP1 and TAZ are highly coexpressed in primary and metastatic GCs

As YAP1 and TAZ have previously been reported to cooperate as transcriptional coactivators in malignancies [6], we examined their expression in GC tumors, compared to normal tissues. As shown in **Figure 1A**, mRNAs for both genes were elevated in GC tumors compared to normal tissues from a TCGA dataset. Interestingly, both genes significantly positively correlated (R=0.42; P value=0, **Figure 1B**) in primary GC tumor tissues (gepia.cancer-pku.cn). Increased expression of YAP1 or TAZ in GC tumor tissues compared to normal was further validated in two independent GC dataset cohorts (GES33335 and GSE146996) (**Figure 1C**; **Figure S1A**), and both YAP1 and TAZ highly correlated in primary GC tissues (**Figure 1D**; **Figure S1B**). The significant correlation of YAP1 and TAZ expression in primary GC tissues was further confirmed in our own tissue microarray (**Figures 1E** and **Figure S1C**) and in another independent GC cohort (GSE237876; **Figure 1F**). Further, in our established 18 patient-derived xenografts (PDXs) from gastroesophageal cancers, both YAP1 and TAZ were highly expressed at the protein (**Figure 1G** and **Figure S1D**) and mRNA (**Figure S1E)** levels.

To determine the expression of YAP1 or TAZ and their correlation in GC peritoneal metastases (GCPMs), dot plots of scRNASeq from 20 GCPM samples revealed that both YAP1 and TAZ are highly expressed and correlated in tumor cell clusters (**Figure 2A**). Among 13 tumor cell clusters, YAP1 and TAZ were highly co-expressed and correlated using tSNE plots (**Figure 2B**). Further, we co-stained YAP1 and TAZ in more than 110 GCPM cases using co-immunofluorescent staining (Co-IF), revealing co-expression of YAP1 and TAZ in most malignant ascites of GCPM samples. As shown by representative staining of both YAP and TAZ in GCPMs (**Figure 2C** and **Figure S2A**), we noticed that both YAP1 and TAZ highly co-localized in the nuclei of malignant ascites tumor cells in GCPMs. Expression of YAP1 and TAZ in GCPM-derived tumor cells was validated using co-IF staining with the tumor marker EpCAM, the stromal marker vimentin, or the macrophage marker CD163 **(Figure S2B**). Furthermore, two independent GC cohorts with peritoneal metastases further confirmed the much higher positive correlation between YAP1 and TAZ (*WWTR1*) in metastatic lesions of GC (GES237876, R=0.70; GSE289037, R=0.89) (**Figure 2D**) than in primary GC cohorts (**Figure 1D,F** and **Figure S1B)**; YAP1 was also significantly higher in GC metastases than primary tumors (**Figure 2E**). Similarly, TAZ expression was significantly increased in GC with peritoneal metastases compared to GC without peritoneal metastasis in an independent

cohort (**Figure S2C).** All these data suggest that both YAP1 and TAZ coexist in GC and highly associate with GCPMs.

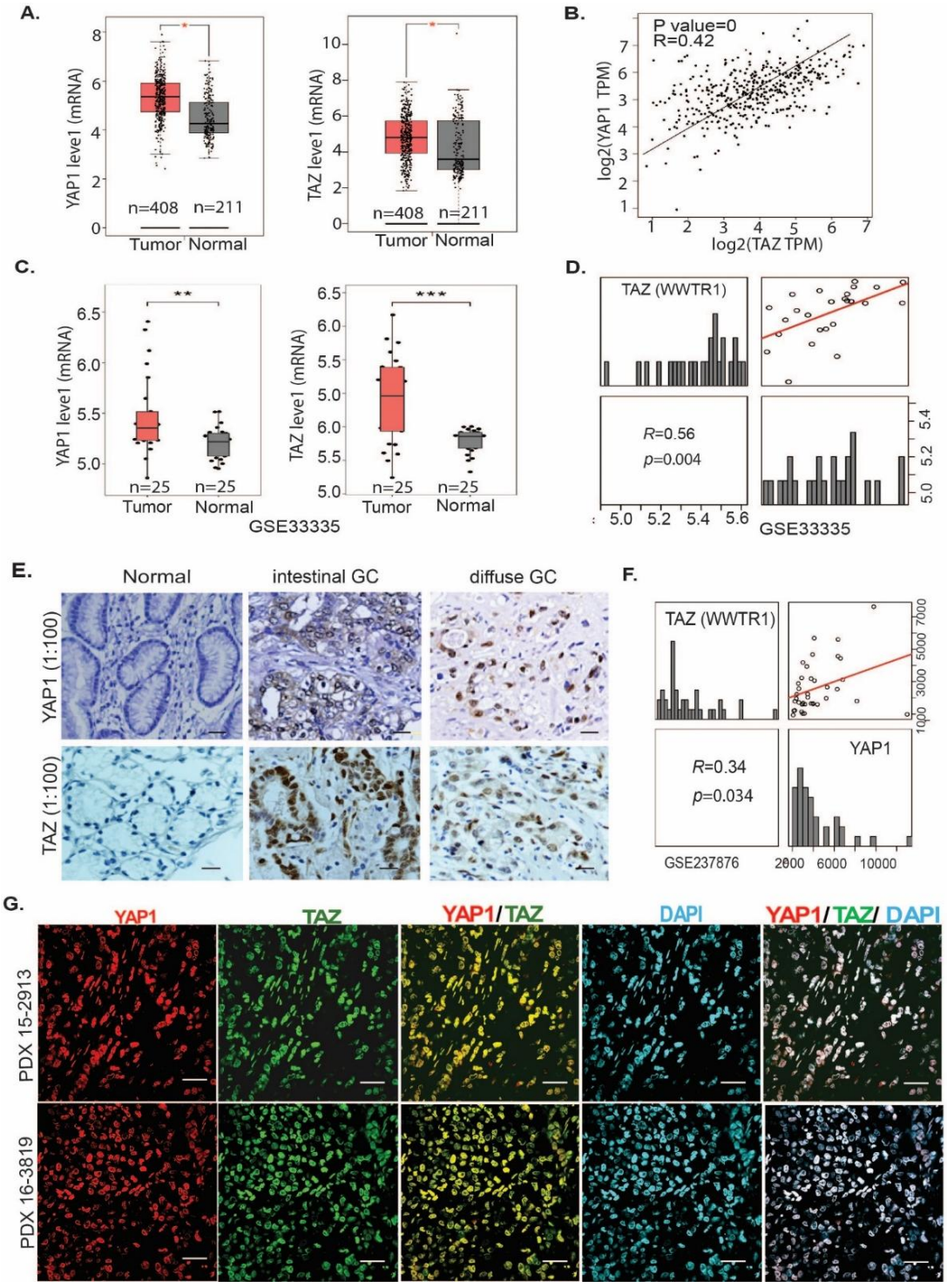

Figure 1. YAP1 and TAZ are highly co-expressed and correlated in primary GC tissues and PDXs. (A) Increased YAP1 or TAZ expression in GC tumor tissues compared to normal tissues (http://gepia.cancer-pku.cn). **(B)** Both YAP1 and TAZ are significantly correlated (R=0.42; *P* value=0). **(C&D)**. Expression of YAP1 or TAZ is significantly higher in GC tumor tissues than normal and significantly positively correlated (R=0.56, *P*=0.004) in the GSE33335 cohort (***P*<0.01; *****P*<0.001); **(E)** Expression of YAP1 or TAZ was determined using immunohistochemistry of 390 GC specimens in both intestinal GC and diffuse GC. **(F)** The correlation of YAP1 and TAZ in GC tissues was further confirmed in an individual GC cohort (GSE237876) (R=0.34, *P*=0.034). **(G)** Colocalization of YAP1 and TAZ in two representative PDXs from GC tissues was determined by co-immunofluorescent staining of YAP1, TAZ, and DAPI (scale bar: 25 μm).

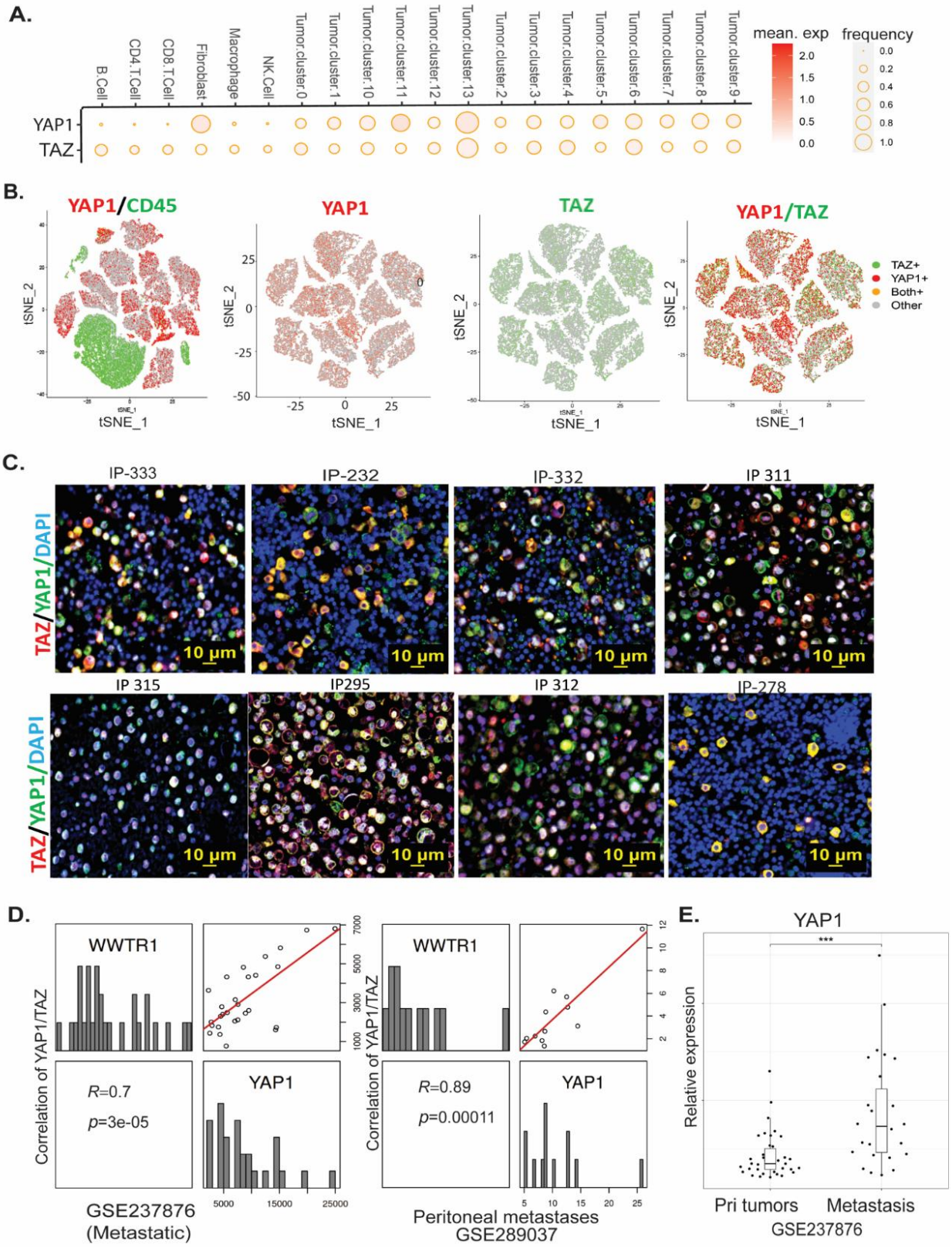

Figure 2. Both YAP1 and TAZ are highly expressed and correlated in metastatic GCPM cells/tissues. (A) Expression of YAP1 and TAZ in tumor cell clusters as shown in dot plots of 20 GCPM samples by scRNAseq. **(B)** Coexpression of YAP1 and TAZ in 13 tumor cell clusters as shown by tSNE plots of GCPM samples by scRNAseq. **(C)** Expression of YAP1 and TAZ, as determined by dual-immunofluorescent staining (co-IF), in representative GCPM samples. Scale bar: 10 μm. **(D)** High correlation of YAP1 and TAZ in two metastatic GC cohorts (GSE237876 and GSE289037). **(E)** Expression of YAP1 was significantly increased in peritoneal metastases compared to primary tumors in a GC cohort (GSE237876).

3.2. YAP1 and TAZ complex with TEAD1-TEAD4 and synergically activate TEAD transcriptional activity

It is well established that during developmental processes, YAP1 and TAZ, which lack DNA-binding capacity, are activated by loss of phosphorylation, translocate to the nucleus, and transactivate target growth genes through their TEAD transcription binding partners. Four TEAD members including TEAD1, TEAD2, TEAD3, and TEAD4 can be utilized by coactivators YAP1 or TAZ or both. However, expression of these TEADs in GCPM and their association with YAP1 or TAZ, and their clinical relevance, are unknown. First, RNAseq analysis in 20 GCPM samples revealed that four TEADs are highly enriched in 13 tumor cell clusters, with TEAD4 enriched in tumor cluster 12 that highly associated with poor survival, while TEAD1 and TEAD2 were also expressed highly in cancer-associated fibroblasts (**Figure 3A**). Further, we revealed that TEAD1-4 are highly increased in GC tumor tissues compared to normal from 2 independent GC cohorts, GES33335 and GES146996 (**Figure S3A,B**). To explore the four TEADs' clinical relevance, we explored the TCGA dataset and found that elevated expression of all four TEADs significantly associated with short GC patient survival, respectively, in GC samples that contain more than 600 cases (**Figure 3B**).

To further detect if TEAD is actively expressed in GCPM samples, we costained TEAD1-TEAD4 and YAP1 using co-immunofluorescent staining (co-IF) in our GCPM specimens and found that the four TEADs were highly expressed and colocalized with YAP1 (**Figure 3C**). In the GSE237876 gastric cancer (GC) cohort comprising metastatic tumors, we observed that **TEAD1, TEAD2, and TEAD4** expression levels were significantly elevated in metastatic tumors compared to primary tumors. **TEAD3** also showed a trend toward higher expression in metastatic tumors; however, this difference did not reach statistical significance (**Figure S3D**). To elucidate the interaction of these TEADs with their co-activator YAP or TAZ, we performed co-immunoprecipitation using either specific YAP1 antibody or TAZ antibody. As shown in **Figure 3D**, an anti-YAP1 antibody coimmunoprecipitated TAZ and TEAD1-TEAD4, with reciprocation shown by anti-TAZ antibody pulldown of YAP1 and TEAD1-TEAD4 (**Figure 3E**), indicating that YAP1 actively interacts with TAZ, and both complex with TEAD1-TEAD4 in two GC cell lines. Functional cooperation of YAP1 and TAZ in GCPMs was shown to occur in transactivation, with combined YAP1 and TAZ overexpression (OE) maximally driving TEAD luciferase activity, compared to OE of YAP1 or TAZ alone, in two GCPM-derived tumor cells (GA0518 and GA0804) and the AGS GC cell line (**Figure 3F**). Co-localization of YAP1 or TAZ with TEADs in representative GCPM samples was further confirmed by co-IF (**Figure S3C**). Altogether, these data suggest that YAP1, TAZ, and TEAD1-TEAD4 are highly expressed and associated in GCPM samples; thus, the YAP1/TAZ/TEADs axis could be a promising therapeutic target in GCPM.

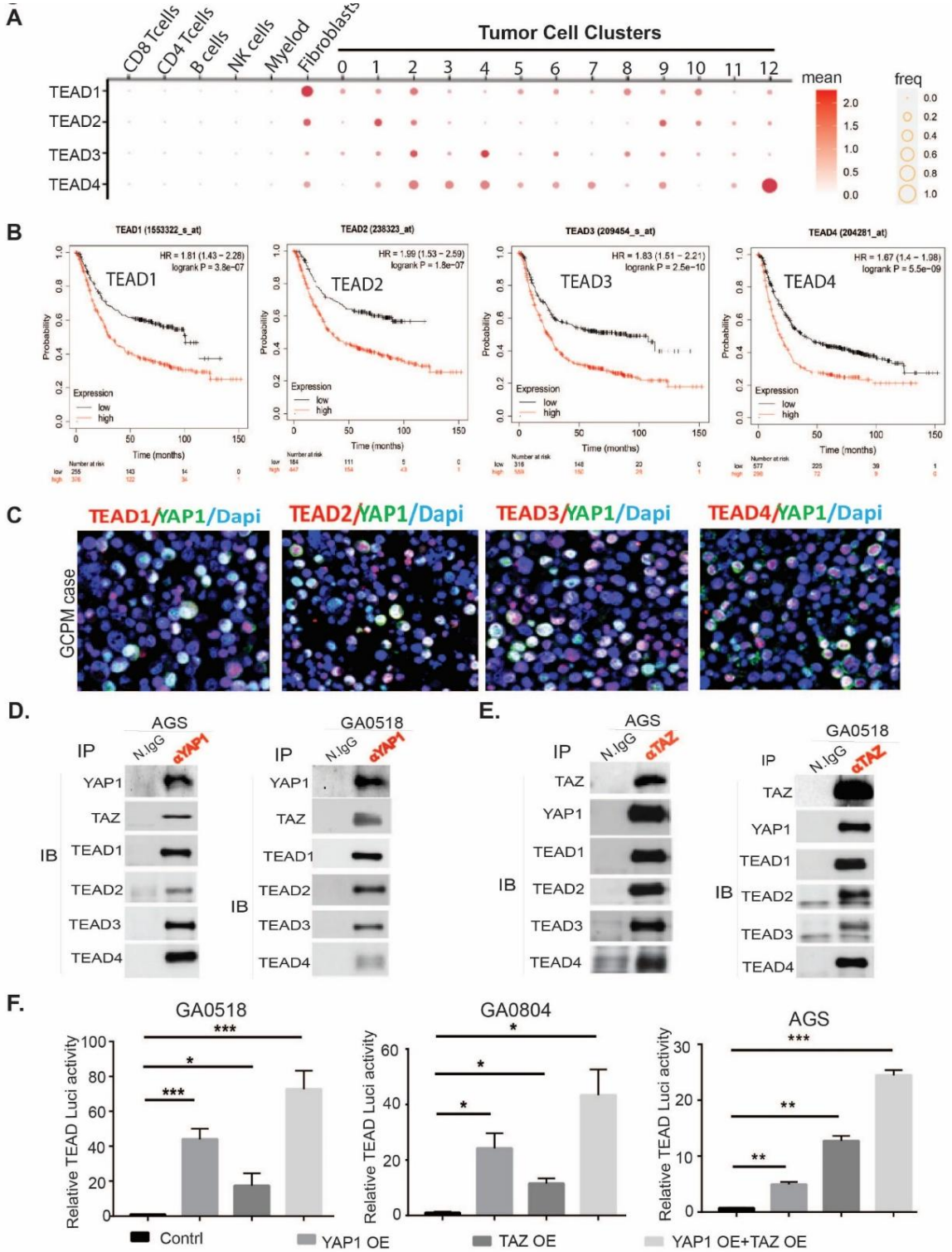

Figure 3. High expression of TEAD1-TEAD4, the transcription factors (TFs) for YAP1/TAZ in GCPM associates with poor survival. (A) scRNAseq showing the expression of TEAD1, TEAD2, TEAD3, and TEAD4 by dot plots from 20 GCPM specimens; **(B)** Association of TEAD1-TEAD4 expression with GC patients' survival in more than 600 advanced GC patients respectively from the TCGA database (kmplot.com). **(C)** Representative GCPM cases stained by dual-immunofluorescence of YAP1 with TEAD1-TEAD4 respectively. **(D)** YAP1 interacts with TAZ and TEAD1-TEAD4 in AGS and GA0518 GC cells as shown by co-immunoprecipitation pulldown using an anti-YAP1 antibody. **(E)** TAZ interacts with YAP1 and TEAD1-TEAD4, as shown by co-immunoprecipitation pulldown using an anti-TAZ antibody in AGS and GA0518 GC cells. **(F)** TEAD transcriptional activity was determined as previously [22] by transient cotransfection of 5X UAS-luciferase reporter and Gal4-TEAD4 with either YAP1cDNA or TAZ cDNA or both in GA0518, GA0804 and AGS cells for 48 hours. *p<0.05, **p<0.01; ***p<0.001.

3.3. YAP1 or TAZ antisense oligos (ASO) effectively suppress each paralog's expression and potently inhibit invasion of patient-derived GCPM cells

We previously showed that in gastroesophageal cancer, inhibition of YAP1 was antitumorigenic, using genetic CRISPR/CAS9 knockout or a pharmacologic inhibitor [5,22]. However, ASOs, which bind specific mRNAs or pre-mRNAs to prevent translation by mRNA degradation or blocked splicing, have the advantages of depletion of the actual protein of interest, minimal off-target effects, and stabilization by chemical modifications, and have now been under preclinical and clinical examination and optimization for over two decades [23-26]. Thus, we examined three distinct ASOs for knockdown of YAP1; ASO#3 was the most efficacious for suppressing YAP1 expression and subsequently inhibiting transactivation of the YAP1 target gene *Cyr61* in both GA0518 and GA084 patient-derived GCPM cells (**Figure 4A-D**). Anti-YAP1 ASOs also dramatically reduced SOX9 and BIRC5, two reported YAP1/TEAD targets, in a dose-dependent manner (**Figure S4**), while also significantly blocking tumor cell invasion in both GA0518 and GA0804 cells (**Figure 4E**). Consistent with YAP1's oncogenic functions, YAP1 ASO effectively inhibited tumor cell proliferation in GA0518 cells, while YAP1 KO clones failed to respond to YAP1 ASO, indicating that YAP1 ASO antitumor effects rely on YAP1 expression (**Figure 4F**). In testing additional YAP1 ASO#10 and YAP1 ASO#11, we found that ASO dramatically reduced colony formation in a dose-dependent manner in GA0804 cells (**Figure S4B**).

Analogously, we assessed the effects of TAZ ASO on TAZ expression. TAZ ASO showed dose-dependent downregulation of TAZ protein (**Figure 5A**) and mRNA (**Figure 5B**) in both GA0518 and GA0804 patient-derived tumor cells. The specificity of TAZ ASO in decreasing TAZ but not YAP1 protein is shown in **Figure S5A** using a dual antibody recognizing both YAP1 and TAZ. Furthermore, we noticed that a TAZ but not a YAP1 ASO significantly downregulated TEAD luciferase activity induced by co-transfection of TAZ and TEAD, indicating that TAZ ASO specifically inhibits TAZ-induced TEAD activation in GA0518 and AGS cells (**Figure 5C**), while both YAP1 or TAZ ASOs significantly reduced YAP1- and TAZ-coactivated TEAD transcriptional activity following co-overexpression of YAP1, TAZ, and TEAD with a UAS luciferase plasmid (**Figure 5D**). In contrast, overexpression of TAZ dramatically increased TEAD transcriptional activity in GA0518 cells (**Figure 5E**). Correspondingly, TAZ ASO dramatically suppressed GC tumor cell invasion in both GA0518 and GA0804 cells (**Figure 5F**). One TAZ ASO (#896558) dramatically reduced an aggressive GA0518 GCPM cells' colony formation as comparable to CA3, a reported potent YAP1/TEAD inhibitor [22] (**Figure S5B,5C**). Altogether, these data support the feasibility of antisense inhibition of YAP1 or TAZ expression and their oncogenic function in GCPMs.

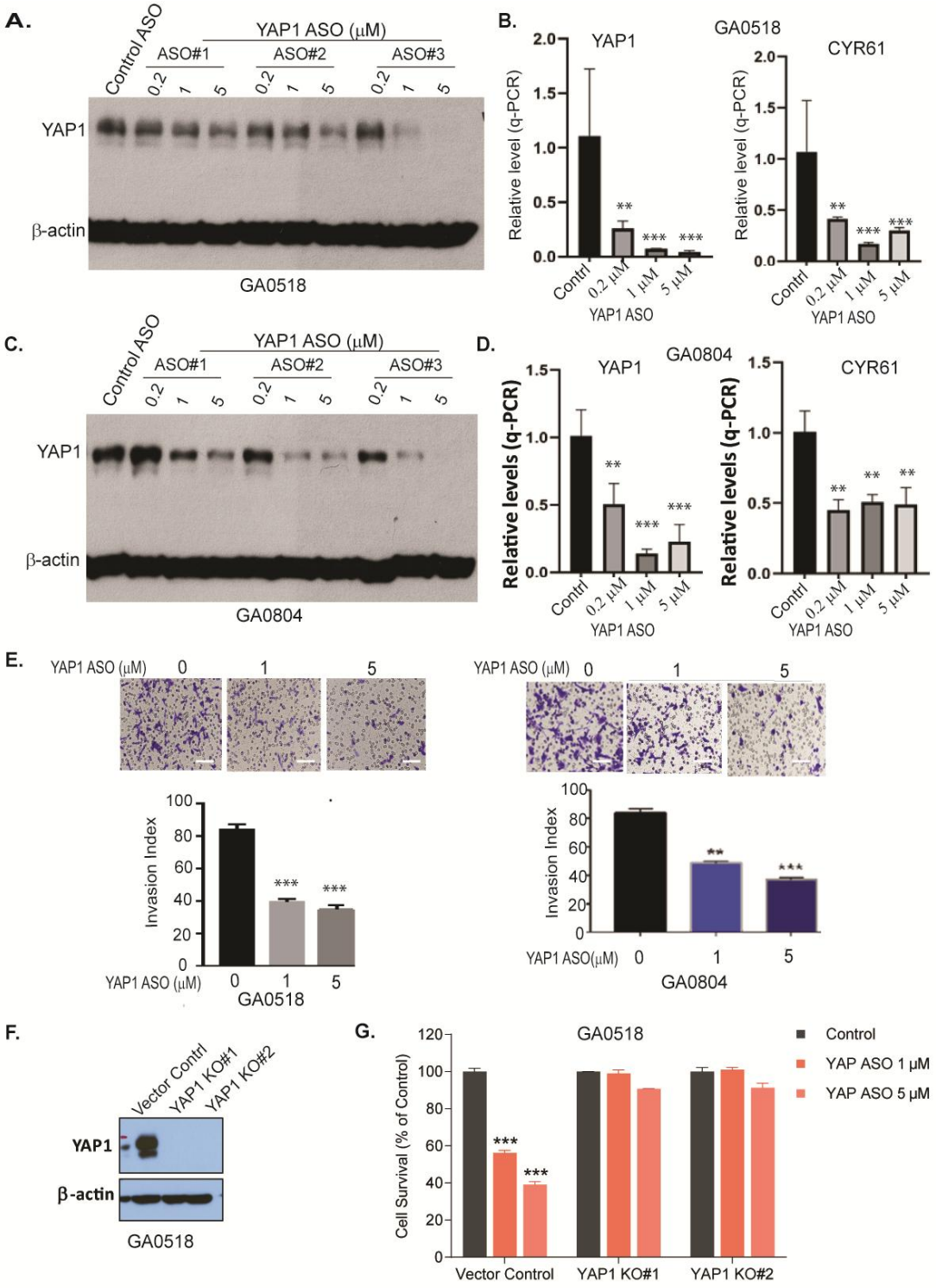

Figure 4. Antisense oligonucleotides (ASOs) of YAP1 specifically suppress YAP1 expression, transcription, and reduce tumor cell malignant behaviors *in vitro*. (A) YAP1 protein was determined by Western blot after 48-hour treatment with YAP1 ASOs in GA0518 cells as indicated; **(B)** YAP1 mRNA (left) and its target CYR61 (right) mRNA levels were dose-dependently decreased by YAP1 ASO as determined by q-PCR in GA0518 cells **p<0.01; ***p<0.001; **(C)** YAP1 protein was determined by Western blot after treatment with YAP1 ASOs in GA0804 cells; **(D)** YAP1 mRNA (left) and its target Cyr61 (right) mRNA levels were decreased by YAP1 ASO as determined by q-PCR in GA0804 cells; **p<0.01; ***p<0.001; **(E)** YAP1 ASO significantly inhibited tumor cell invasion in both GA0518 (left) and GA0804 (right) GCPM tumor cells. Lower panels, quantification. **p<0.01; ***p<0.001; **(F)** Expression of YAP1 was detected by Western blot showing YAP1 knockout efficiency; **(G)** Cell survival was detected by MTS assay in GA0518 cells with or without YAP1 KO treated with YAP1 ASO at different dosages. ***p<0.001

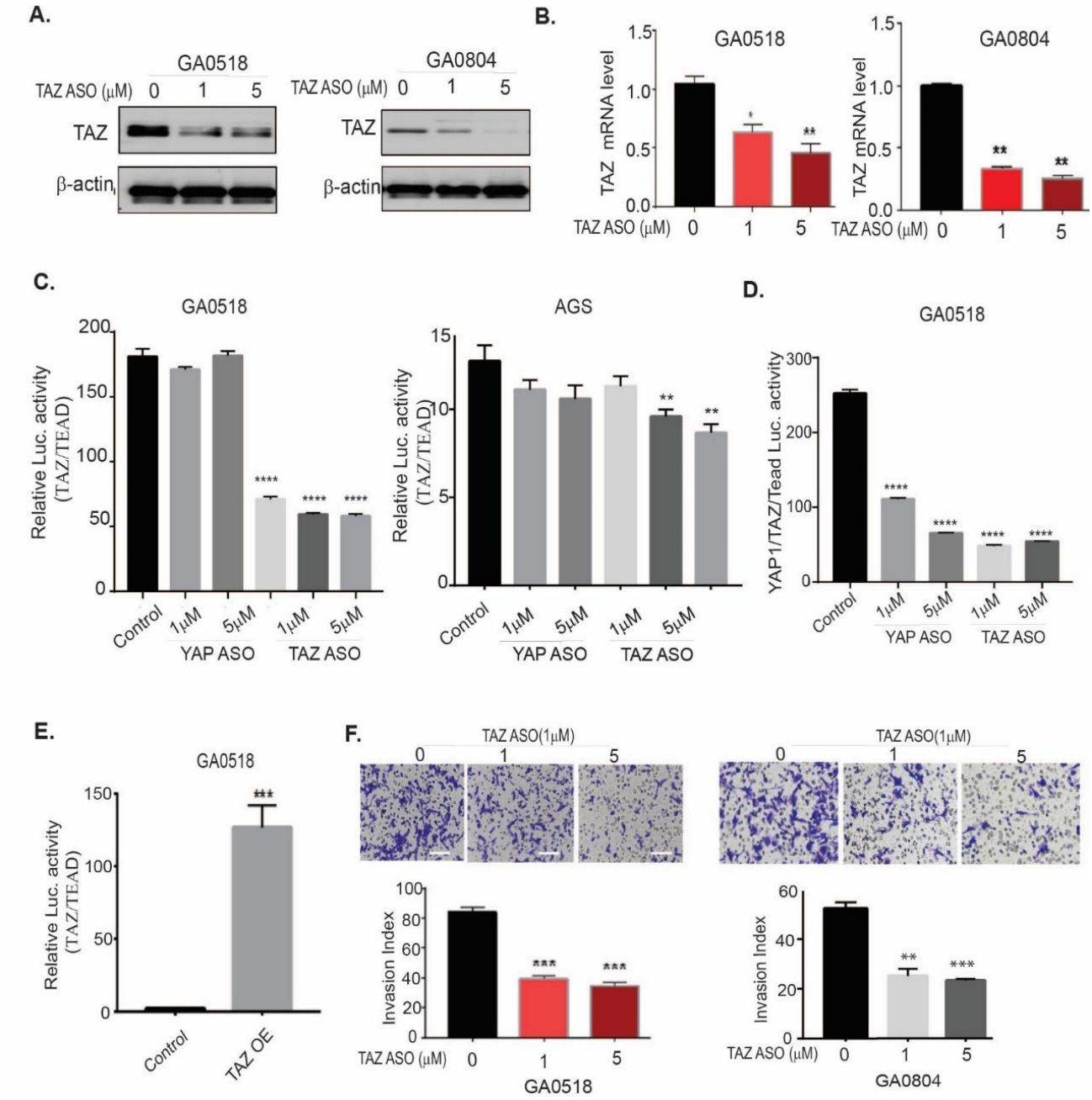

Figure 5. TAZ ASO suppresses TAZ expression, transcription, TAZ/TEAD transcriptional activity, and reduces tumor cell invasion, *in vitro*. (A&B) TAZ protein and mRNA levels were decreased by TAZ ASO as determined by Western blot and q-PCR in both GA0518 and GA0804 cells; *p<0.05, **p<0.01; **(C)** TAZ/TEAD transcriptional activity was determined as previously [22] by transient cotransfection of 5X UAS-luciferase reporter and Gal4-TEAD4 with either TAZ cDNA or YAP1cDNA in GA0518 and GA0804 cells for 48 hours. *p<0.05, **p<0.01; ****p<0.001. **(D**) Luciferase activity of YAP1/TAZ/TEAD was determined after cotransfection of 5X UAS-luciferase reporter and Gal4-TEAD4 with both TAZ cDNA and YAP1cDNA and then treated with YAP1 ASO or TAZ ASO in GA0518 cells; ****p<0.001; **(E)** Luciferase activity of TAZ/TEAD was determined after cotransfection of 5X UAS-luciferase reporter and Gal4-TEAD4 with TAZ cDNA overexpression, as done previously. ***p<0.001; **(F)** TAZ ASO strongly suppressed tumor cell invasion capacity in a dose-dependent manner in both GA0518 (left) and GA0804 (right) cells. **p<0.01; ***p<0.001.

3.4. YAP1 depletion upregulates TAZ and enhances TAZ interactions with TEAD4 and the AP-1 heterodimer of C-JUN/FOSB

While transcriptional regulation of YAP1 and TAZ is complex, involving crosstalk with numerous pathways, we and others [15] have shown that in addition to

binding TEAD transcription factors, YAP1/TAZ can interact with other transcription factors/mediators such as STAT3, β-Catenin, Notch, BRD4, SMAD3, and AP-1 to mediate their oncogenic functions [9,12-14,27,28]. Consequently, inhibition of TEAD alone may be insufficient, as YAP1 or TAZ can engage alternative transcription factors to drive target gene expression, even though current therapeutic approaches targeting the Hippo/YAP1/TEAD axis remain focused on TEAD inhibition [29-31]. However, how YAP1 inhibition influences TAZ interaction with its binding partners in GCPMs is unclear. One could hypothesize that depletion of YAP1 could be compensated by upregulation of TAZ and increased TAZ binding to other TFs in addition to TEAD, and vice versa. As shown in **Figure 6A**, genetic YAP1 knock out (KO) upregulated TAZ protein and mRNA in GA0518 cells. Similarly, ASO inhibition of YAP1 increased TAZ protein and mRNA levels in both GA0518 and GA0804 cells (**Figure 6B**). Interestingly, using co-immunoprecipitation, we found that YAP1 genetic KO or YAP1 ASO treatment in GA5018 cells dramatically increased TAZ complexation with TEAD4 (but not TEAD1) and the AP-1 heterodimer (c-JUN and FOSB) (**Figure 6C&6D**). Consequently, we focused specifically on the TEAD4 family member, with co-localization of TAZ and TEAD4 further validated in our representative GCPM specimen (**Figure 6E**). Moreover, upregulation of TEAD4 and AP-1 heterodimers c-JUN and FOS-B upon YAP1 depletion in GA0518 cells was further validated using co-IF (**Figure 6F**). These results indicate that YAP1 depletion either by genetic KO or ASO pharmacological inhibition upregulates TAZ and increases its binding to TEAD4 and the AP-1 components c-JUN and FOSB, facilitating GC progression and metastasis. This may explain why targeting YAP1 alone in clinical trials failed, thus providing rationale for combination therapeutic strategies against GCPMs.

3.5. Combined inhibition of YAP1 and TAZ represses their expression and suppresses tumor cell malignant behaviors *in vitro*

Previous studies showed that combined inhibition of YAP1 and TAZ was necessary to prevent blastocyst formation (*versus* either protein alone), during embryonic development [32], and repression of hepatocellular tumorigenesis [15]. Consequently, we assessed whether this combination could maximally repress each paralog's expression and function in GC cells. As depicted in **Figure 7A-D**, YAP1 ASO treatment alone dose-dependently decreased YAP1 protein and mRNA in GA0518 cells (**Figure 7A&7B**), while complementarily increasing TAZ protein and mRNA levels as mentioned earlier. Vise versa, ASO inhibition of TAZ alone dramatically decreased TAZ protein and mRNA levels, while increasing YAP1 expression in both GA0518 and GA0804 cells. However, combined ASO inhibition of YAP1 and TAZ reduced both mRNA and protein expression of YAP1, TAZ, and their targets BIRC5 and Snail in both cell lines (**Figure 7A&7C** and **Figure S6A**). Correspondingly, combined ASO inhibition of YAP1 and TAZ dramatically reduced tumor cell malignant behaviors including tumor cell invasion and colony formation (**Figures 7E&7F**), and the combined inhibition of both YAP1 and TAZ elicited the best anti-tumor cell proliferation effects in $YAP1^{high}$ GA0518 and GA0804 patient-derived tumor cells, but less so in $YAP1^{null}$ MKN45 cells (**Figure S6B-D**). These data indicate that co-targeting YAP1 and TAZ is the best strategy to treat GCPMs with hyperactivation of Hippo/YAP1/TAZ signaling.

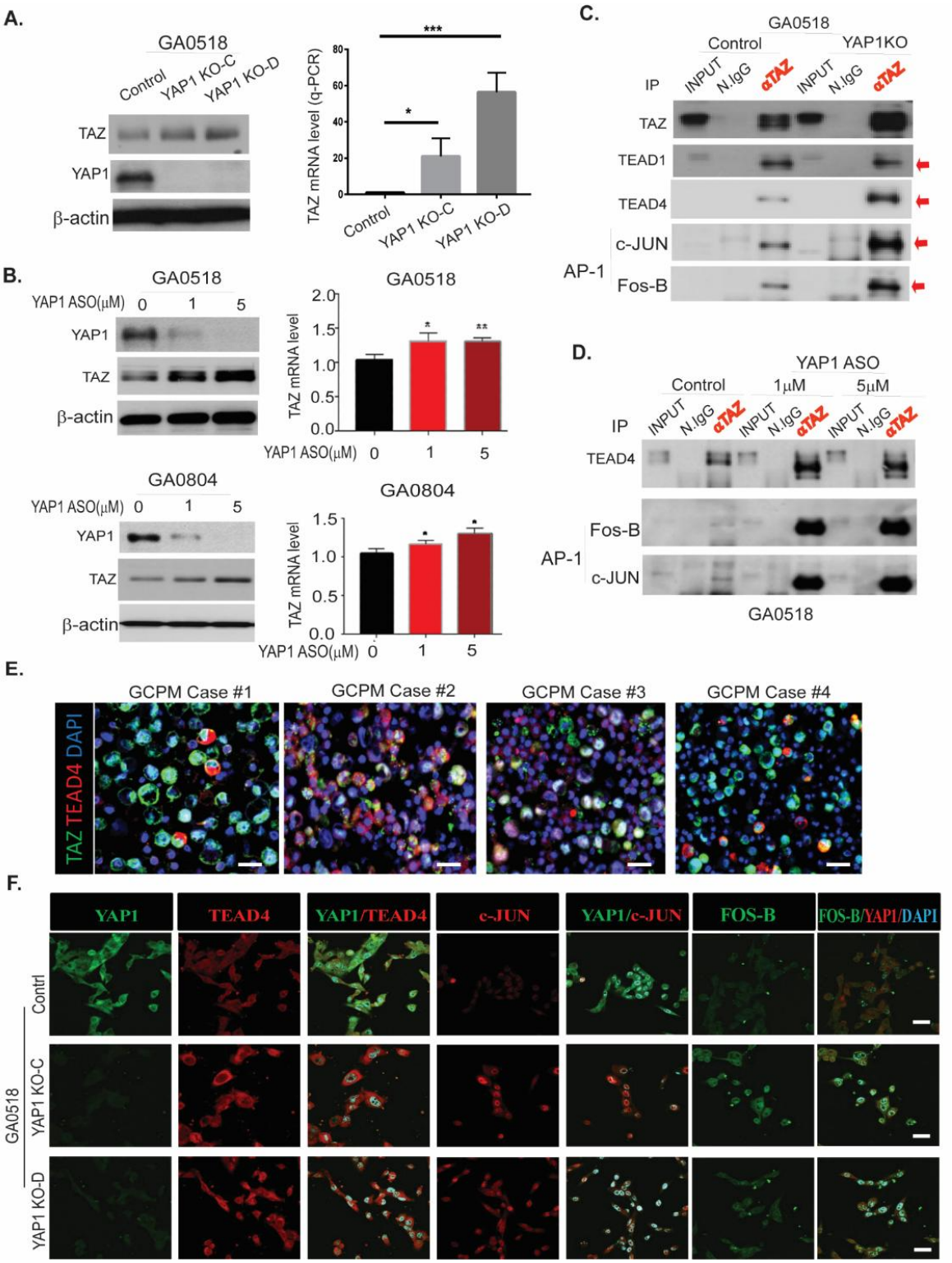

Figure 6. Inhibition of YAP1 by Lenti-CRISPR/CAS9 or YAP1 ASO increases TAZ expression, transcription, and binding to TEAD4 and the AP-1 heterodimer C-Jun/FOSB in GC cells. (A) TAZ level increased upon YAP1 KO by Western blot (left) and q-PCR (right) in GA0518 cells; **(B)** YAP1 ASO decreased YAP1 but increased TAZ protein (left) and mRNA (right) levels in both GA0518 (above) and GA0804 (below) cells by Western blot and q-PCR, respectively; **(C)** YAP1 KO dramatically increased TAZ binding to TEAD4 and the AP1 heterodimer of C-JUN and FOSB as determined by co-IP in GA0518 cells; **(D)** Similarly, inhibition of YAP1 by ASO increased TAZ binding to TEAD4 and the AP1 heterodimer of C-JUN and FOSB as determined by co-IP in GA0518 cells. **(E)** Co-IF staining of TAZ and TEAD4 in four representative GCPM specimens. Scale bar: 25 μm. **(F)** Expression of YAP1, TEAD4, c-JUN, and FOS-B was determined by co-IF using their specific antibodies, respectively, in GA0518 YAP1 KO clones compared to GA0518 Control cells. Scale bar: 20 μm.

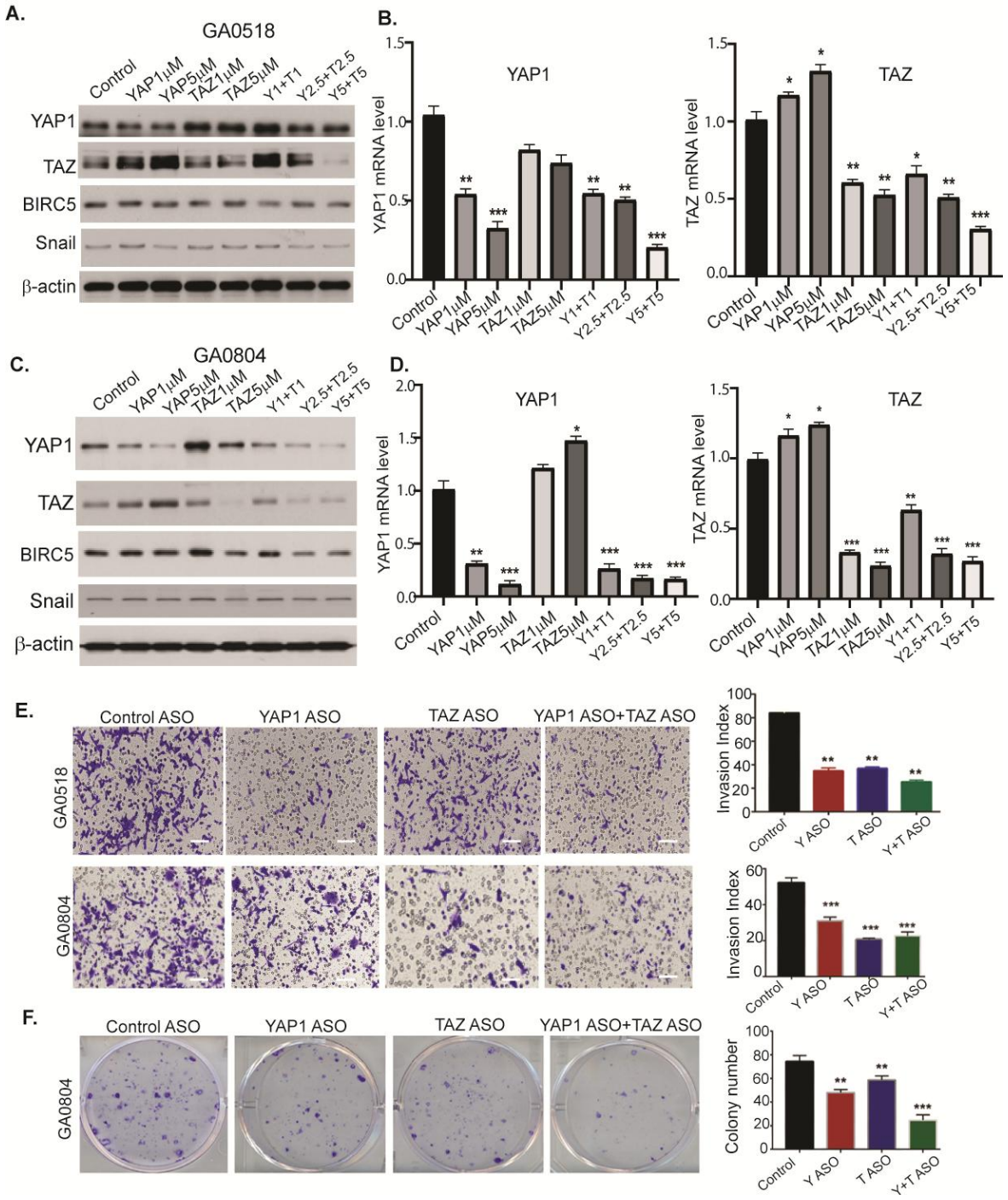

Figure 7. **ASO co-targeting of YAP1 and TAZ dramatically suppresses both YAP1 and TAZ expression and tumor cell invasion and colony formation in patient-derived GCPM cells. (A-D)** YAP1 and TAZ protein and mRNA levels were determined by western blot and q-PCR upon 48-hour treatment with YAP1 ASO or TAZ ASO or their combination in both GA0518 and GA0804 cells. *p<0.05, **p<0.01; ***p<0.001. **(E)** Invasion capacity was determined by western blot and q-PCR upon treatment of YAP1 ASO or TAZ ASO or their combination in both GA0518 and GA0804 cells. **p<0.01; ***p<0.001; Scale bar: 25 μm; **(F)** Colony formation was determined in GA0804 cells upon treatment with YAP1 ASO or TAZ ASO or their combination. **p<0.01; ***p<0.001.

3.6. Co-targeting YAP1 and TAZ suppresses tumor progression and enhances anti-PD1 immune therapy *in vivo*

To determine the antitumor effects of ASO co-inhibition of YAP1 and TAZ *in vivo*, we used an established GA0518 PDX line that highly expresses both YAP1 and

TAZ (**Figure S2B**). We injected patient-derived GA0518 PDX line cells subcutaneously and treated mice using YAP1 ASO (40mg/kg, 5 times a week), TAZ ASO (40 mg/kg, 5 times a week), or their combination (YAP1 ASO 20 mg/kg + TAZ ASO 20 mg/kg). After three weeks of treatment, tumor weights were significantly reduced by the combined YAP1 ASO and TAZ ASO treatments, compared to either alone or control cells (**Figure 8A**). Similarly, tumor volumes were significantly reduced in a time-dependent manner, with a YAP1 ASO and TAZ ASO combination providing the greatest inhibition (**Figure 8B**). Moreover, while the YAP1 or TAZ ASO groups greatly reduced the expression of YAP1 or TAZ, respectively, and the KI67 proliferation marker, the combination YAP1 and TAZ co-targeting group most suppressed YAP1 and TAZ expression and KI67+ proliferating populations (**Figure 8C**). Independent similarly designed experiments treating additional PDXs using different YAP1 and TAZ ASOs consistently revealed that the combination of YAP1 ASO and TAZ ASO demonstrated the best anti-tumor effects over either treatment alone (**Figure S7A&S7B**). The expressions of YAP, TAZ, epithelial tumor marker EpCAM, and stromal marker vimentin were dramatically reduced by the combination treatment (**Figure S7C**). Furthermore, we preliminarily observed that YAP1 ablation using genetic knockout or ASO treatment in GC tumor cells significantly increased PD-L1 expression (**Figure S8A&S8B**), a finding whose mechanisms are currently under active investigation in our laboratory. Thus, we hypothesized that combining YAP1 inhibition with anti-PD-1 immunotherapy would yield superior antitumor activity. Accordingly, we treated KP-Luc2 syngeneic mice with an anti-YAP1 ASO together with the checkpoint inhibitor anti-PD-1, and found the combination to be the most efficacious, producing the greatest reduction in tumor volume. This regimen also suppressed the cancer stemness marker SOX9 and the proliferation marker Ki67, strongly reduced YAP1 expression, and increased CD8 T-cell infiltration (**Figures 8D,E**). Collectively, these results demonstrate the antitumorigenic effect of combined YAP1/TAZ inhibition and support the potential efficacy of co-targeting YAP1 and PD-1.

4. Discussion

Peritoneal metastasis (PM; malignant ascites or implants) in GC patients (GCPM) is common and poses a challenge with short survival and lack of effective therapeutics. In this study, using scRNAseq and immunofluorescent staining, we observed that both YAP1 and TAZ and their transcriptional factors TEAD1-TEAD4 are highly expressed in GCPM tumor cells; high expression of these proteins also associated with poorer prognosis. Further, we note that recently developed YAP1 or TAZ ASOs can effectively and specifically suppress YAP1 or TAZ expression and transcription accompanied by decreased tumor cell invasion, colony formation, and cell proliferation in YAP1/TAZ high GC cells. Interestingly, ASO inhibition of YAP1 or TAZ alone could complementarily increase the other at the protein and mRNA levels. Moreover, we showed that genetic or pharmacological inhibition of YAP1 enhanced TAZ expression and activity and increased its interaction with TEAD4 and the AP-1 heterodimer (c-JUN/FOSB). Simultaneous ASO inhibition of YAP1 and TAZ reduced both YAP1 and TAZ proteins and mRNA levels and their downstream targets while significantly decreasing proliferation and invasive capacity of YAP1-high tumor cells. Most importantly, co-targeting YAP and TAZ by ASOs significantly

attenuated tumor progression and GCPM in the PDX model, sensitized tumors to anti-PD1 immunotherapy, and enhanced CD8 T cell infiltration in the KP-Luc syngeneic model. Taken together, our studies open a new avenue for developing a novel therapeutic strategy of ASO co-targeting of both YAP1 and TAZ in GCPMs.

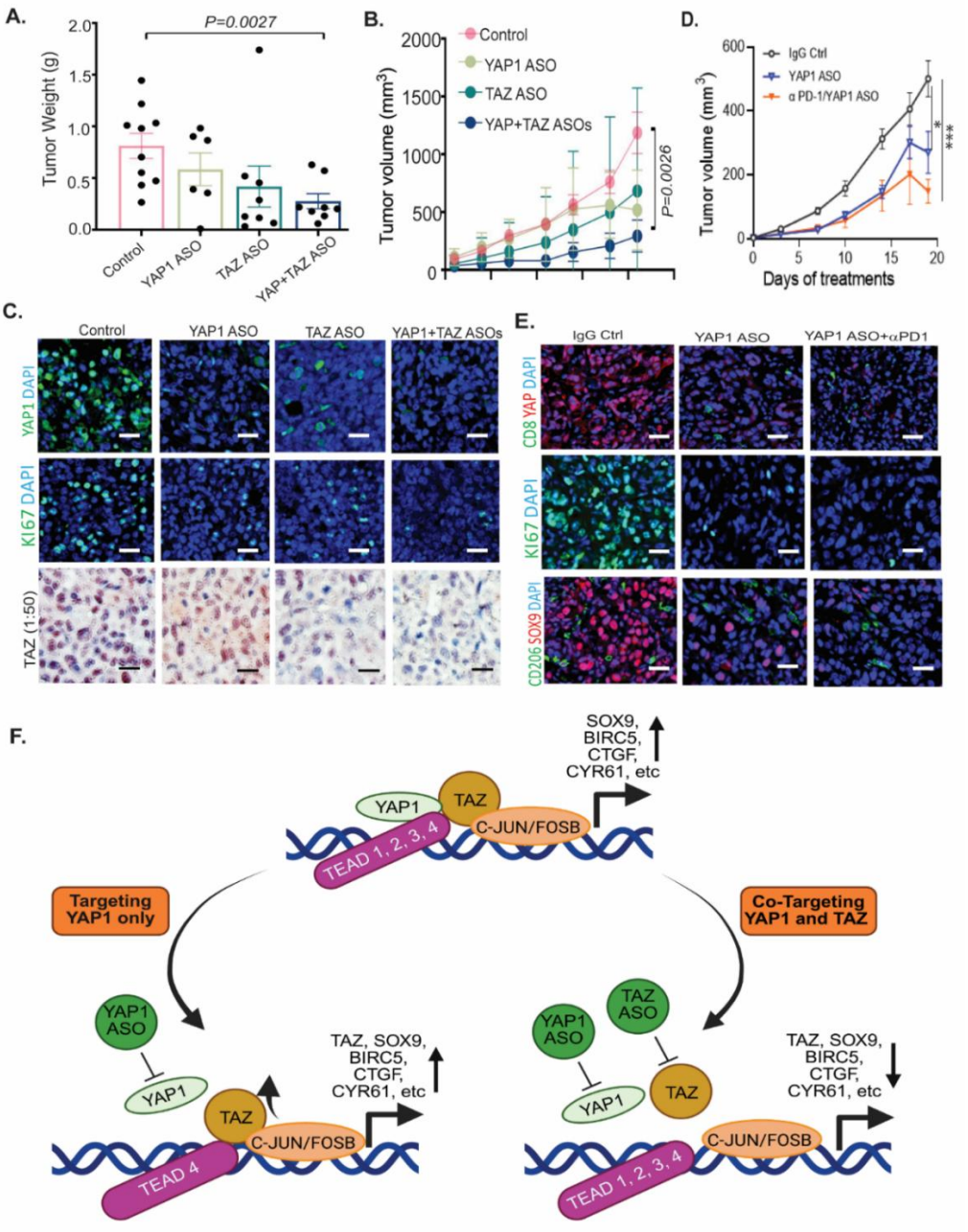

Figure 8. **ASO co-targeting of YAP and TAZ significantly attenuated tumor growth in PDX and enhanced tumor immunity in the KP-Luc syngeneic model. (A-B)** Combined ASO inhibition of YAP1 and TAZ suppressed tumor weights and volumes in the GA0518 PDX model; YAP1 ASO or TAZ ASO: 50mg/kg, 5 times a week for three weeks. **(C)** Expression of YAP1, TAZ, and KI67 as determined by IF staining or immunohistochemistry in YAP1, TAZ, or combination ASO-treated PDX tumors; Scale bar: 20 μm; **(D)** Combined treatment of YAP1 ASO and anti-PD1 antibody had greater antitumor effects than YAP1 ASO alone or the control group; *p<0.05, ***p<0.001; YAP1 ASO 50mg/kg, 5 times a week, IP injection; anti-PD1 antibody, 2 times a week, iv injection, for three weeks. **(E)** Expressions of YAP1, KI67 and SOX9 were decreased by YAP1 ASO alone and the combination treatment YAP1 ASO/anti-PD1, while CD8 infiltration was increased and CD206 M2 macrophages were decreased. Scale bar: 20 μm; **(F)** Working model and the rationale for co-targeting YAP1 and TAZ in advanced GCPM patients.

Dysregulation of the Hippo signaling pathway (with failure to regulate YAP1 and its paralog TAZ) associates with numerous phenotypes of malignant disease, including the epithelial-to-mesenchymal transition (EMT), angiogenesis, and generation of cancer stem cells [6]. With 46% identity, YAP1 and TAZ have been traditionally accepted as interchangeable [7]. However, a handful of studies have suggested differing, malignancy-specific roles in tumor progression, with TAZ (*versus* YAP1) preferentially overexpressed in hepatocellular carcinoma (HCC) [15] and the two proteins playing disparate roles in kidney function [33]. In another study of gastric cancer cells, using YAP1 or TAZ overexpression combined with knockout of the paralog, although numerous similar target genes/functions were found (including platelet signaling and lipoprotein formation), YAP1 expression distinctly associated with cell-substrate junctions [34]. Consequently, one could hypothesize that in many cases, the combined effects of both proteins, *versus* either alone, would be additive or synergistic. Indeed, it was shown that the combination of YAP1 and TAZ inhibition was necessary to suppress blastocyst formation during embryonic development [32], and for maximal inhibition of tumorigenicity in HCC cells [15]. Likewise, both YAP1 and TAZ were required for liver regeneration in a genetically engineered mouse model [35]. Although studies have largely focused on YAP1 function in tumor progression and metastasis, we believe that TAZ is equally important in mediating tumor cell malignant behaviors in GC. However, it is thus far less clear if both YAP1 and TAZ coactivators co-exist in GCPMs and how both cooperate to mediate tumor growth and metastasis. In this study, our findings revealed that both YAP1 and TAZ highly coexist and correlate in GCPM specimens, and overexpression of both YAP1 and TAZ in GC cell lines synergistically increased TEAD transcriptional activity. Combined inhibition of YAP1/TAZ was necessary for maximal downregulation of each, while also most greatly suppressing GC neoplastic phenotypes, providing a strong rationale for co-targeting both YAP1 and TAZ coactivators in GCPMs with highly activated YAP1/TAZ/TEAD signaling.

Recently, numerous attempts have emerged to develop TEAD inhibitors from academia or pharma to combat activation of Hippo/YAP1 TAZ/TEAD signaling, with several undergoing clinical trials (NCT04665206; NCT05228015). However, when inhibiting TEAD transcriptional factors, the Hippo co-activators YAP1 or TAZ might utilize other transcriptional factors to facilitate tumor cell survival, progression, and metastasis. It has been reported that YAP1/TAZ can cooperate with other signaling molecules and bind other TFs such as Wnt/β-catenin, Notch, STAT3, AP-1, and TGF-β/SMAD to mediate their oncogenic and metastatic potential [7,9-13]. Furthermore, while most Hippo/YAP1/TEAD-targeting strategies have focused on inhibition of YAP1, it is possible that this might be insufficient, due to possible upregulation of TAZ. A recent clinical trial (NCT04659096) targeting YAP1 alone using an YAP1 antisense oligo (ION537) [36] in advanced solid tumors was terminated due to toxicity and lack of efficacy in advanced solid tumors. Indeed, our findings revealed that TAZ expression and activity increased upon YAP1 inhibition, and TAZ strongly interacted with TEAD4 and the AP-1 heterodimer c-JUN and FOSB to increase their downstream targets that facilitate GC cell growth and metastasis.

A potential interpretation of our findings, supported by coimmunoprecipitation, dual luciferase assays, qRT-PCR, and Western blot, is depicted in **Figure 8F**. In this scenario, during tumor progression, YAP1 and TAZ complex with TEAD

transcriptional factors (TEAD1-TEAD4) to elicit target gene (*e.g.*, CYR61, CTGF, BIRC5, SOX9) expression (top). Inhibition of YAP1 alone using YAP1 ASO upregulates TAZ, possibly via an AP-1 feed forward loop, to maintain tumorigenicity (*e.g.*, proliferation, stemness, EMT). This could occur via increased TAZ binding to TEAD4 and the AP-1 heterodimer c-JUN and FOSB (lower left), while combined YAP1 and TAZ inhibition reduce both YAP1 and TAZ binding to TEAD1-TEAD4 and AP-1 TFs to downregulate target genes and cancerous traits (lower right). While others have demonstrated YAP1 compensation following TAZ knockdown [15], we believe we are the first to demonstrate the reciprocal effect, *i.e.*, TAZ upregulation following YAP1 suppression. Moreover, while the mechanism of TAZ upregulation, by YAP1 depletion, remains unclear, a feed-forward loop for YAP1/TAZ via AP-1 signaling was previously shown in uveal melanoma [37]; our demonstration of AP-1/TAZ complexation would suggest that this could also positively reinforce TAZ expression.

In summary, the ancient Hippo pathway, discovered in a screen for tumor inhibitors [6], plays an integral role in cancers of the gastrointestinal tract [38]. While the Hippo effector YAP1 has been intensely investigated as a therapeutic target, we found the expression and activation of its paralog TAZ to be critical to maintaining tumorigenic phenotypes, especially upon YAP1 depletion, thus diminishing anti-YAP1 efficacy. Further, in targeting TEADs alone, as currently emerging in preclinical and clinical phases, the Hippo coactivators YAP1 or TAZ might utilize other TFs such as AP-1, BRD4, STAT3, *etc*. Thus, simultaneously targeting both the YAP1 and TAZ oncoproteins could allow for maximal tumor suppression, therefore warranting further study of such combinations in both preclinical and clinical studies.

Supplementary Materials

The following supplementary materials are available on the website of this paper: CHP2603010003SupplementaryMaterials.zip.

1. Figure S1. YAP1 and TAZ are highly expressed and significantly correlated in GC tumor tissues and PDXs.
2. Figure S2. Co-expression of YAP1 and TAZ in representative GCPM samples.
3. Figure S3. High expression of TEAD1-TEAD4, the transcription factors (TFs) for YAP1/TAZ, in primary tumor and metastatic tissues.
4. Figure S4. Effects of YAP1 ASO on YAP1 targets and on tumor cell colony formation.
5. Figure S5. TAZ ASO specifically suppress TAZ expression and inhibit GA0518 cell colony formation.
6. Figure S6. Cotreatment GC tumor cells using YAP1, and TAZ ASOs effectively suppress both YAP1 and TAZ expression and suppress tumor cell growth in YAP1-high GC cells.
7. Figure S7. ASO co-targeting of YAP and TAZ significantly attenuated tumor growth in an additional PDX.
8. Figure S8. YAP1 ablation by genetic knock out or ASO in GC tumor cells increased PDL-1 expression.
9. Table S1. Primers used in this study.
10. Table S2. Antibodies used in this study for Western blot, Immunoprecipitation, and Immunofluorescent staining.

Abbreviations

The following abbreviations are used in this manuscript:

GC: Gastric cancer; GCPM: gastric cancer peritoneal metastasis; YAP1: Yes-associated protein 1; TAZ: Transcriptional co-Activator with PDZ-binding motif; ASO: antisense oligonucleotide; TEAD1-4: TEA domain transcription factors 1–4; EMT: epithelial-to-mesenchymal transition; KO: genetic knockout; OE: overexpression; LATS1/2: large tumor suppressor kinases1/2; DMSO: dimethyl sulfoxide; IHC: Immunohistochemistry; scRNAseq: Single-cell RNA sequencing; HCC: hepatocellular carcinoma; PDX: Patient-derived xenograft; TCGA: The Cancer Genome Atlas

Declarations

Ethics Statement

Animal protocol (ID: 23-016) and all animal experiments were approved by the Institutional Animal Care and Use Committee (IACUC) from Cooper University Hospital and conducted in compliance with relevant ethical guidelines.

Human subject protocols involved in this study were approved from the Institutional Review Board of The University of Texas MD Anderson Cancer Center (IRB0531), the Cooper-Coriell Cancer Biobank (IRB CCCB0001), and Camden Cancer Research Center. Human studies entailed immunohistochemistry staining of de-identified patient tissues to determine expression of YAP1, TAZ, TEADs, and other proteins. Similarly, human cancer cells from de-identified patients were used in culture and in the aforementioned PDX models.

Consent to participate

All participants provided informed written consent. All patients who volunteered to provide research specimens provided written informed consent for participation in this study using an approved document.

Consent for publication

All patient samples were de-identified such that consent for publication was not applicable

Availability of Data and Material

The raw sequence data reported in this paper have been deposited and published previously (GUT 2020; Nature Medicine 2021). Data are available in a public, open access repository.

Funding

This work was supported by grants from the NIH (R01 CA269685), DOD (CA210457 and CA230323), and the New Jersey Commission on Cancer Research (NJCCR) (COCR26RBG006).

Competing interests

The authors declare no competing interests.

Author contributions

All authors are responsible for the overall content as guarantors, and all authors revised and approved the final version of the manuscript. Conception and, design: SS and JAA; Draft the manuscript: SS, CB; development of methodology, acquisition of data (performed experiments, analyzed data): JW, DA, JZ, GZ, YF, YZ, JZ, MG, AP, GC, AS, SS, XY, MP, SS; acquired and managed patients, provided facilities, resources, PDXs and other support: CV, VK, SZ, TY, SD, RS, FS, GG, JA, SS ; Analysis and interpretation of data: AP, GC, JZ, SS.

Acknowledgements

We thank Ionis Pharmaceuticals, Inc. for kindly providing the YAP1 and TAZ ASOs used in this study.

References

1. Bray F, Laversanne M, Sung H, Ferlay J, Siegel RL, Soerjomataram I, et al. Global cancer statistics 2022: GLOBOCAN estimates of incidence and mortality worldwide for 36 cancers in 185 countries. CA Cancer J Clin. 2024;74(3):229-263. DOI
2. Siegel RL, Kratzer TB, Giaquinto AN, Sung H, Jemal A. Cancer statistics, 2025. CA Cancer J Clin. 2025;75(1):10-45. DOI
3. Cronin KA, Scott S, Firth AU, Sung H, Henley SJ, Sherman RL, et al. Annual report to the nation on the status of cancer, part 1: National cancer statistics. Cancer. 2022;128(24):4251-4284. DOI
4. Mithany RH, Shahid MH, Manasseh M, Saeed MT, Aslam S, Mohamed MS, et al. Gastric Cancer: A Comprehensive Literature Review. Cureus. 2024;16(3):e55902. DOI
5. Ajani JA, Xu Y, Huo L, Wang R, Li Y, Wang Y, et al. YAP1 mediates gastric adenocarcinoma peritoneal metastases that are attenuated by YAP1 inhibition. Gut. 2021;70(1):55-66. DOI
6. Piccolo S, Dupont S, Cordenonsi M. The biology of YAP/TAZ: hippo signaling and beyond. Physiol Rev. 2014;94(4):1287-1312. DOI
7. Pocaterra A, Romani P, Dupont S. YAP/TAZ functions and their regulation at a glance. J Cell Sci. 2020;133(2):jcs230425. DOI
8. Fu M, Hu Y, Lan T, Guan KL, Luo T, Luo M. The Hippo signalling pathway and its implications in human health and diseases. Signal Transduct Target Ther. 2022;7(1):376. DOI
9. Park HW, Kim YC, Yu B, Moroishi T, Mo JS, Plouffe SW, et al. Alternative Wnt Signaling Activates YAP/TAZ. Cell. 2015;162(4):780-794. DOI
10. Hu S, Molina L, Tao J, Liu S, Hassan M, Singh S, et al. NOTCH-YAP1/TEAD-DNMT1 Axis Drives Hepatocyte Reprogramming Into Intrahepatic Cholangiocarcinoma. Gastroenterology. 2022;163(2):449-465. DOI
11. Gruber R, Panayiotou R, Nye E, Spencer-Dene B, Stamp G, Behrens A. YAP1 and TAZ Control Pancreatic Cancer Initiation in Mice by Direct Up-regulation of JAK-STAT3 Signaling. Gastroenterology. 2016;151(3):526-539. DOI
12. Sadhukhan P, Feng M, Illingworth E, Sloma I, Ooki A, Matoso A, et al. YAP1 induces bladder cancer progression and promotes immune evasion through IL-6/STAT3 pathway and CXCL deregulation. J Clin Invest. 2024;135(2). DOI
13. Nishio M, Sugimachi K, Goto H, Wang J, Morikawa T, Miyachi Y, et al. Dysregulated YAP1/TAZ and TGF-beta signaling mediate hepatocarcinogenesis in Mob1a/1b-deficient mice. Proc Natl Acad Sci U S A. 2016;113(1):E71-80. DOI
14. Totaro A, Castellan M, Di Biagio D, Piccolo S. Crosstalk between YAP/TAZ and Notch Signaling. Trends Cell Biol. 2018;28(7):560-573. DOI
15. Hayashi H, Higashi T, Yokoyama N, Kaida T, Sakamoto K, Fukushima Y, et al. An Imbalance in TAZ and YAP Expression in Hepatocellular Carcinoma Confers Cancer Stem Cell-like Behaviors Contributing to Disease Progression. Cancer Res. 2015;75(22):4985-4997. DOI

16. Song S, Xu Y, Huo L, Zhao S, Wang R, Li Y, et al. Patient-derived cell lines and orthotopic mouse model of peritoneal carcinomatosis recapitulate molecular and phenotypic features of human gastric adenocarcinoma. J Exp Clin Cancer Res. 2021;40(1):207. DOI
17. Okazaki S, Shintani S, Hirata Y, Suina K, Semba T, Yamasaki J, et al. Synthetic lethality of the ALDH3A1 inhibitor dyclonine and xCT inhibitors in glutathione deficiency-resistant cancer cells. Oncotarget. 2018;9(73):33832-33843. DOI
18. Wang R, Song S, Qin J, Yoshimura K, Peng F, Chu Y, et al. Evolution of immune and stromal cell states and ecotypes during gastric adenocarcinoma progression. Cancer Cell. 2023;41(8):1407-1426 e1409. DOI
19. Song S, Honjo S, Jin J, Chang SS, Scott AW, Chen Q, et al. The Hippo Coactivator YAP1 Mediates EGFR Overexpression and Confers Chemoresistance in Esophageal Cancer. Clin Cancer Res. 2015;21(11):2580-2590. DOI
20. Song S, Maru DM, Ajani JA, Chan CH, Honjo S, Lin HK, et al. Loss of TGF-beta adaptor beta2SP activates notch signaling and SOX9 expression in esophageal adenocarcinoma. Cancer Res. 2013;73(7):2159-2169. DOI
21. Fan Y, Li Y, Yao X, Jin J, Scott A, Liu B, et al. Epithelial SOX9 drives progression and metastases of gastric adenocarcinoma by promoting immunosuppressive tumour microenvironment. Gut. 2023;72(4):624-637. DOI
22. Song S, Xie M, Scott AW, Jin J, Ma L, Dong X, et al. A Novel YAP1 Inhibitor Targets CSC-Enriched Radiation-Resistant Cells and Exerts Strong Antitumor Activity in Esophageal Adenocarcinoma. Mol Cancer Ther. 2018;17(2):443-454. DOI
23. Li Y, Song S, Pizzi MP, Han G, Scott AW, Jin J, et al. LncRNA PVT1 Is a Poor Prognosticator and Can Be Targeted by PVT1 Antisense Oligos in Gastric Adenocarcinoma. Cancers (Basel). 2020;12(10):2995. DOI
24. Dhuri K, Bechtold C, Quijano E, Pham H, Gupta A, Vikram A, et al. Antisense Oligonucleotides: An Emerging Area in Drug Discovery and Development. J Clin Med. 2020;9(6):2004. DOI
25. Lauffer MC, van Roon-Mom W, Aartsma-Rus A, Collaborative N. Possibilities and limitations of antisense oligonucleotide therapies for the treatment of monogenic disorders. Commun Med (Lond). 2024;4(1):6. DOI
26. Hu Y, Revenko A, Barsoumian H, Bertolet G, Fowlkes NW, Maazi H, et al. Inhibition of MER proto-oncogene tyrosine kinase by an antisense oligonucleotide enhances treatment efficacy of immunoradiotherapy. J Exp Clin Cancer Res. 2024;43(1):70. DOI
27. Song S, Li Y, Xu Y, Ma L, Pool Pizzi M, Jin J, et al. Targeting Hippo coactivator YAP1 through BET bromodomain inhibition in esophageal adenocarcinoma. Mol Oncol. 2020;14(6):1410-1426. DOI
28. Kim MK, Han SH, Park TG, Song SH, Lee JY, Lee YS, et al. The TGFbeta-->TAK1-->LATS-->YAP1 Pathway Regulates the Spatiotemporal Dynamics of YAP1. Mol Cells. 2023;46(10):592-610. DOI
29. Tang TT, Konradi AW, Feng Y, Peng X, Ma M, Li J, et al. Small Molecule Inhibitors of TEAD Auto-palmitoylation Selectively Inhibit Proliferation and Tumor Growth of NF2-deficient Mesothelioma. Mol Cancer Ther. 2021;20(6):986-998. DOI
30. Hagenbeek TJ, Zbieg JR, Hafner M, Mroue R, Lacap JA, Sodir NM, et al. An allosteric pan-TEAD inhibitor blocks oncogenic YAP/TAZ signaling and overcomes KRAS G12C inhibitor resistance. Nat Cancer. 2023;4(6):812-828. DOI
31. Sabnis RW. Novel Indazole Compounds as TEAD Inhibitors for Treating Cancer. ACS Med Chem Lett. 2023;14(10):1334-1335. DOI
32. Sasaki H. Roles and regulations of Hippo signaling during preimplantation mouse development. Dev Growth Differ. 2017;59:12-20. DOI
33. Varelas X. The Hippo pathway effectors TAZ and YAP in development, homeostasis and disease. Development. 2014;141(8):1614-1626. DOI
34. Lee Y, Finch-Edmondson M, Cognart H, Zhu B, Song H, Low BC, et al. Common and Unique Transcription Signatures of YAP and TAZ in Gastric Cancer Cells. Cancers (Basel). 2020;12(12):3667. DOI
35. Lu L, Finegold MJ, Johnson RL. Hippo pathway coactivators Yap and Taz are required to coordinate mammalian liver regeneration. Exp Mol Med. 2018;50(1):e423. DOI

36. Macleod RA. Abstract ND11: The discovery and characterization of ION-537: A next generation antisense oligonucleotide inhibitor of YAP1 in preclinical cancer models. Cancer Res. 2021;81(13_Supplement): ND11. DOI
37. Koo JH, Plouffe SW, Meng Z, Lee DH, Yang D, Lim DS, et al. Induction of AP-1 by YAP/TAZ contributes to cell proliferation and organ growth. Genes Dev. 2020;34(1-2):72-86. DOI
38. Shibata M, Ham K, Hoque MO. A time for YAP1: Tumorigenesis, immunosuppression and targeted therapy. Int J Cancer. 2018;143(9):2133-2144. DOI